Proposal for Observing XUV-Induced Rabi Oscillation Using Superfluorescent Emission

Jun Jie Cui,[1] Yongjun Cheng,[1] Xin Wang,[1] Zheng Li,[2,3,4] Nina Rohringer,[5] Victor Kimberg,[6,*] and Song Bin Zhang[1,†]
[1]School of Physics and Information Technology, Shaanxi Normal University, Xi'an 710119, China
[2]State Key Laboratory for Mesoscopic Physics and Collaborative Innovation Center of Quantum Matter, School of Physics, Peking University, Beijing 100871, China
[3]Collaborative Innovation Center of Extreme Optics, Shanxi University, Taiyuan, Shanxi 030006, China
[4]Peking University Yangtze Delta Institute of Optoelectronics, Nantong, Jiangsu 226010, China
[5]Center for Free-Electron Laser Science CFEL, Deutsches Elektronen-Synchrotron DESY, Notkestraße 85, 22607, Hamburg, Germany
[6]Theoretical Chemistry and Biology, Royal Institute of Technology, Stockholm 10691, Sweden

(Received 28 February 2023; accepted 2 June 2023; published 25 July 2023)

Intense x-ray and extreme ultraviolet (XUV) light sources have been available for decades, however, due to weak nonlinear interaction in the XUV photon energy range, observation of Rabi oscillation induced by XUV pulse remains a very challenging experimental task. Here we suggest a scheme where photoionization of a He medium by an intense XUV pump pulse is followed by a strong population inversion and Rabi oscillation at the $He^+(1s-3p)$ transition and is accompanied by superfluorescence (SF) of the 7.56 eV pulse at the $He^+(3p-2s)$ transition. Our numerical simulations show that the Rabi oscillation at the $He^+(1s-3p)$ transition induced by an XUV pulse with photon energy 48.36 eV results in significant signatures in the SF spectra, allowing us to identify and characterize the XUV induced Rabi-oscillatory regime. The proposed scheme provides a sensitive tool to monitor and control ultrafast nonlinear dynamics in atoms and molecules triggered by intense XUV.

DOI: 10.1103/PhysRevLett.131.043201

Rabi oscillation [1,2] is one of the key concepts in quantum optics and strong field light-matter interactions. This phenomenon, consisting in a periodic modulation of level populations in a two-level system, has been broadly observed and applied for optical and microwave coherent controls in many fields [3–10], and also becomes increasingly important in quantum computing and quantum information processing [11–14]. However, it is challenging to observe Rabi oscillation in the short wavelength x-ray and extreme ultraviolet (XUV) regime [15,16], where the nonlinear light-matter interaction is strongly suppressed as compared to that in the optical and microwave regime.

In spite that the intense short XUV pulses are available already for decades from free-electron laser (FEL) sources [17–20], and many theoretical predictions are proposed to measure Rabi oscillation at short wavelengths using electron spectra [21–26], the first direct experimental observation of Rabi oscillation in the XUV wavelength has just been achieved in 2022 with the help of photoelectrons emission spectroscopy in He atoms [16]. Because of this, versatile methods sensitive to the nonlinear phenomena induced by short-wavelength pulses are highly required.

A prominent possibility to register Rabi oscillation is related to the observation of emission spectra affected by the XUV nonlinear effect on an adjacent transition. In the x-ray range, theoretical predictions of the stimulated emission both in atoms [27] and molecules [28,29] showed that the spectral changes induced on strong x-ray field driven transitions are rather small due to small transition dipole moments, thus limiting the observation of the Rabi oscillation. In the ultraviolet and XUV regime, where the nonlinear interaction is stronger, the amplified fluorescence has drawn broad interest [30–36]. Theoretical [30–33] and experimental [34–36] studies confirmed the presence of the collective emission effect as superfluorescence (SF) in singly and doubly excited atoms.

An effect of modified Rabi frequency on SF in the presence of an intense laser has been theoretically discussed decades ago [37], followed by demonstration of SF and the ringing spectral phenomena in semiconductor lasers [38], discussion of SF in lasing without inversion conditions [39], and SF in photonic crystals [40]. These preceding studies of SF on optical and XUV transitions [33–40] proposed that the SF emission spectra manifest a ringing effect related to the Rabi oscillation on the emission channel, and that the SF spectra can also be modified in the presence of a strong control pulse. However, an explicit reflection of Rabi oscillations induced by XUV radiation in the SF emission spectra was not yet discussed. Recalling that the ringing structure of SF spectra in the strongly oscillatory SF regime depends on the density of excited atoms [41–44], one may conjecture that the Rabi oscillations induced by an intense XUV pulse influence the SF spectra, as the strong field varies sufficiently the excited state population.

In the present Letter we propose and explore theoretically a scheme, where the Rabi oscillations induced by the pump XUV pulse is fingerprinted by spectral changes in SF

spectra on an adjacent transition. The helium atom is a good candidate to showcase many important observations by XUV pulses [16,34,35]; we consider He atom gas pumped by an ultrashort intense XUV pulse at 48.36 eV photon energy. The pump pulse ionizes the He medium and induces Rabi oscillation on the $He^+(1s-3p)$ resonant transition. The pump process is followed by photon emission on the $He^+(3p-2s)$ transition at 7.56 eV, triggering SF along the gas medium, whose spectrum reflects $He^+(1s-3p)$ Rabi oscillation at the pumped transition. In contrast to the conventional way of direct excitation to He doubly excited state by XUV pulse, the proposed scheme allows us to prevent the effect of a doubly excited state, and the spectral emission channel can be easily identified. And the SF is observed at the UV spectral range free from the background of the high intensity XUV pump pulse. Variation of the pump intensity changes the Rabi oscillation of the population between $He^+(1s)$ and $He^+(3p)$ states, resulting in a significant splitting, broadening, and shifting for the spectral features of the SF spectral profile at the $He^+(3p-2s)$ transition, as we show below. The proposed scheme provides a convenient measure in order to characterize the Rabi oscillation in the XUV regime.

We consider an XUV pump pulse at photon energy 48.36 eV irradiating an 1 mm long He gas medium in its ground state $|g\rangle$ [see Fig. 1(a)]. The pump ionizes the He atomic ensemble and promotes it to the excited state $He^+(3p)|i\rangle$ with lifetime $\tau_i = 329$ ps, which decays to the final state $He^+(2s)|f\rangle$ by emitting a photon of 7.56 eV or back to the ground state $He^+(1s)|0\rangle$. Our simulations of the discussed processes are based on the solution of the one-dimensional Maxwell-Bloch equation, which is described in detail in Supplemental Material (SM), Note 1 [45]. The pump pulse is assumed to have a 30 fs Gaussian envelope with various peak intensities in $10^{12}-10^{15}$ W/cm^2. Because of the stochastic nature of spontaneous emission, the simulations were averaged over 20 single shots.

Figure 1(b) shows the pump intensity dependent population (right after the pump pulse) of the four considered states of He and He^+ at the end of the gas medium ($Z = Z_0 = 1$ mm): He ground state ρ_{gg}, He^+ ground state ρ_{00}, excited state ρ_{ii}, and the final state ρ_{ff}. Here we use a gas pressure of 700 Pa (atomic density $N \approx 1.7 \times 10^{23}$ m^{-3}). The oscillations between $He^+(1s)$ and $He^+(3p)$ populations approach 0.5 at the high pump intensities, which clearly indicates the transition saturation and Rabi oscillation induced by the pump pulse. The pump intensities I_p for local minima and maxima in the occupation ratio between $He^+(1s)$ and $He^+(3p)$ are selected and labeled, corresponding to n and $n+1/2$ complete Rabi cycles, respectively [26]. The population dynamics at the end of the medium is almost identical to ones at $Z = 0$ mm [26], which shows negligible absorption of the pump pulse

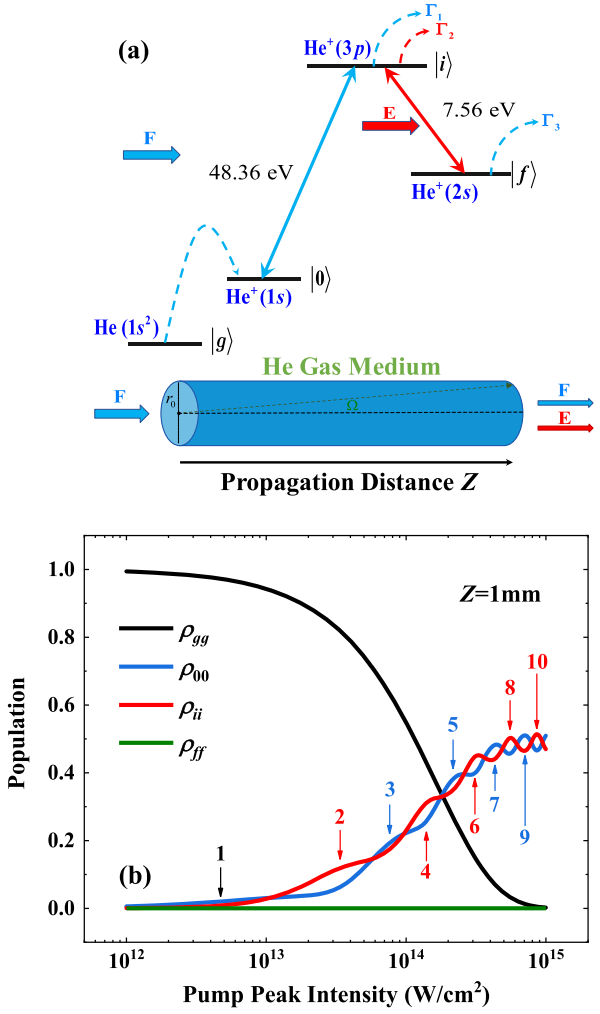

FIG. 1. (a) Scheme of the studied transitions in He and He^+, as well as illustration of the propagation of the pump XUV field F and emitted SF field E. Here $\Gamma_{1,3}$ and Γ_2 show photoionization channels by the pump and emitted radiation, respectively (see SM, Table S1 [45]). (b) Population of the four states (right after the pump pulse), shown in panel (a), at $Z = Z_0 = 1$ mm as a function of the pump intensity; the labels correspond to 4.7 (1), 34 (2), 76 (3), 140 (4), 220 (5), 310 (6), 430 (7), 550 (8), 710 (9), and $860(10) \times 10^{12}$ W/cm^2.

in the present case. Indeed, the maximal dissipation of the pump energy after the propagation is less than 6%. The low pump absorption and thus strong pump pulse propagating through the entire medium ensure the high population inversion ratio up to the end of the gas cell, creating favorable conditions for nonlinear effects and cooperative emission process, such as SF.

Using the selected benchmark pump intensities I_p, that correspond to n and $n+1/2$ complete Rabi cycles, we simulate propagation of the pump and emitted radiation through the medium. Figure 2(a) presents a temporal profile of the SF at the end of the medium $Z = Z_0 = 1$ mm at different I_p. It shows that rising of the pump intensity allows the SF process to develop from the damped SF

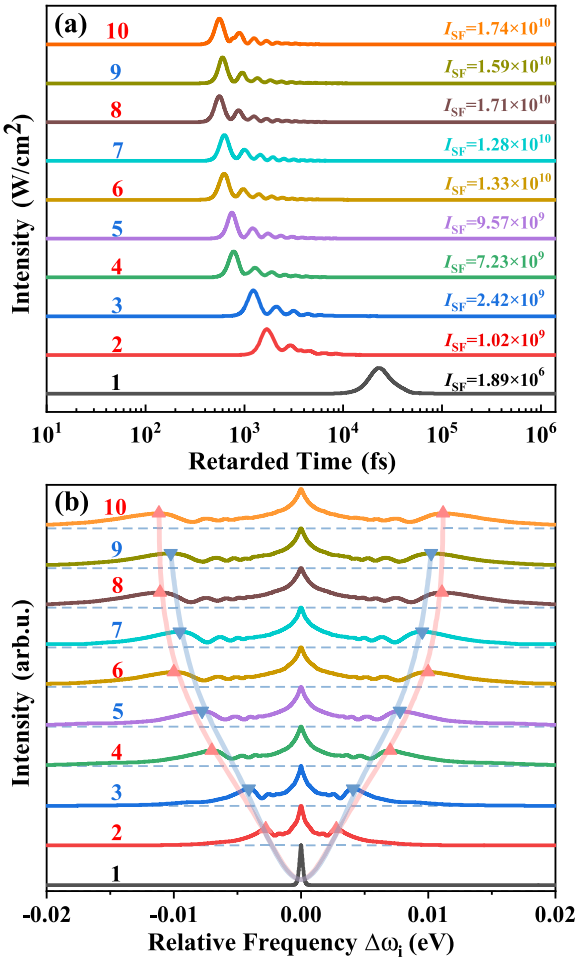

FIG. 2. Temporal (a) and spectral (b) dependence of the $He^+(3p-2s)$ SF on the pump intensities [labels 1–10 correspond to the pump intensities identified in Fig. 1(b)]. The peak values I_{SF} (in W/cm^2) for the SF intensity are given in panel (a). All the results are averaged over 20 pulses in the simulation.

regime to strongly oscillatory SF regime (see SM, Note 2 [45]). The strong oscillatory SF manifests in shortening of the emitted pulse duration, decrease of the delay time between the pump and the main peak of the SF pulse train (retarded time), as well as in the increase of the oscillation amplitude, in full agreement with a previous study for the strongly oscillatory SF [31]. When I_p is larger than 5.5×10^{14} W/cm^2, ρ_{ii} reaches the saturation, and the difference between temporal profiles of SF becomes minor [see Fig. 2(a)].

The SF spectral profiles [Fig. 2(b)] are obtained by the Fourier transform of the SF electric field for each individual propagation and then averaged over 20 realizations in order to account probably for the stochasticity of the SF process. Obviously, increase of the pump intensity leads to gradual broadening and splitting of the spectral line from a single peak to multipeak structure. Such a splitting could be resolved by the grating based spectrometer, whose resolving power is more than 10^4 in the vacuum ultraviolet region 4–12 eV [57]. The spectral splitting increases along with the growth of the pump intensity until it reaches the saturation regime at $I_p > 5.5\times10^{14}$ W/cm^2. One can see, that the spectral splitting shows oscillatory behavior as it is outlined by the blue downward pointing triangles and red triangles in Fig. 2(b). The oscillation pattern is remarkably similar to the evolution of ρ_{ii} shown in Fig. 1(b) modulated by the Rabi cycling. The SF corresponding to local maxima of ρ_{ii} [I_p labeled as 2, 4, 6, 8, 10 in Fig. 1(b)] have a larger splitting [see red triangles in Fig. 2(b)], as compared to those corresponding to local minima of ρ_{ii} [I_p labeled as 1, 3, 5, 7, and 9 in Fig. 1(b) and blue inverted triangles Fig. 2(b)]. Note that the XUV pulse from the seeded FEL with stable pulse duration and intensity is suggested for experimental observation of the predicted effect. A minor 10% fluctuation of the pump intensity would not smear the spectral structures shown in Fig. 2(b), as it follows from our estimation based on intensity-dependent population analysis in the saturation regime [Fig. 1(b)]. However, strong temporal and spectral fluctuations of the self-amplified spontaneous emission (SASE) x-ray free-electron laser (XFEL) pulse would smear the spectra and thus the SASE pulse is not suggested for the first experiment. In other words, the oscillation and saturation of the splitting of SF are the results of Rabi oscillation between states $He^+(1s)$ and $He^+(3p)$ as well as saturation of the $He^+(1s-3p)$ transition induced by the pump pulse, and can be used to analyze the population dynamics of the excited state.

This can be explained by the fact that SF formation is inherently coupled to the formation of macroscopic polarization during the propagation through the gas medium prepared by the pump pulse. SF is a cooperative spontaneous radiation process, it depends crucially on the dephasing time T_{DP} from both the collision dephasing and Doppler broadening effect (see SM, Note 3 [45]). The SF shows temporal oscillation or a ringing effect, as a result of the cooperative emission process [41–44], which can be classified based on the relative values of the dephasing time T_{DP}, the cooperation time τ_r and the delay time of SF pulse τ_D. For $T_{DP} > \tau_D$, the dephasing has little effect on the coherence formation, resulting in the SF emission. Furthermore, when the total number of excited particles N_i is larger than the maximum number of cooperatively radiating atoms N_c, atoms undergo strong reabsorption and reemission processes, strongly oscillatory SF can occur, which exhibits a temporally ringing structure (see SM, Note 2 [45]). The present cases are exactly in the strongly oscillatory region, so that the excited population directly determines the magnitude of the ringing structure, as well as SF spectral profiles. The higher population of the excited state and the larger density of excited atoms naturally favor the SF formation. In other words, if the dephasing time is comparable or even shorter than the cooperative emission

time or the medium is thin, no enough amplification can be gained, the emission spectra would be located in the damped SF and amplified spontaneous emission region; no significant ringing effect will be observed in the emission spectra, the minor splitting and changes of the spectral profiles would limit the observation of Rabi oscillation.

Two cases of high pump intensities $I_p = 5.5 \times 10^{14}$ W/cm^2 and 7.1×10^{14} W/cm^2 [eighth and ninth pump intensity in Fig. 1(b)] are analyzed in more detail to understand the propagation dynamics. For $I_p = 5.5 \times 10^{14}$ W/cm^2, one can find that $T_{\mathrm{DP}} = 14$ ps, $\tau_D = 0.48$ ps, $N_c = 5.11 \times 10^8$, and $N_i = 1.67 \times 10^{11}$ (see SM, Note 2 [45]), $N_i \gg N_c$ so that SF shows the strongly oscillatory regime. This analysis is supported by the ringing effect of the SF temporal profile obtained in the simulations (Fig. 2). The SF computed for various gas pressures (see SM, Note 5 [45]) also supports that the SF is in a strong oscillatory regime. Further increase of the pump intensity to 7.1×10^{14} W/cm^2 results in slight decrease of SF intensity and increase of the pulse delay time [Fig. 2(a)]. This is explained by the Rabi cycling effect on the $|0\rangle - |i\rangle$ transition, which causes little reduction of the excited state population ρ_{ii} [see populations at eighth and ninth pump intensity in Fig. 1(b)], creating less favorable conditions for SF formation with longer characteristic time τ_r and delay time τ_D. So the XUV-induced Rabi oscillation at the $\mathrm{He}^+(1s-3p)$ transition changes the population of state $\mathrm{He}^+(3p)$, which determines the magnitude of SF ringing structures and the Autler-Townes effect at the $\mathrm{He}^+(3p-2s)$ transition.

The temporal profiles of the populations for the two above mentioned pump intensities are shown in Figs. 3(a) and 3(b), respectively. Temporal evolution of the populations can be classified into three parts: the first 200 fs dominated by the pump pulse [the pump pulse is centered at 100 fs (see SM, Note 1 [45])]; the SF formation in 200 fs–100 ps; and the spontaneous emission for the time > 100 ps. In the first time interval of 200 fs, the pump pulse saturates the transition $|0\rangle - |i\rangle$ and generates Rabi oscillations of ρ_{00} and ρ_{ii} (see insets of Fig. 3). In the final period of spontaneous emission, the population of the excited state decays continuously to the ionic $\mathrm{He}^+(1s)$ and $\mathrm{He}^+(2s)$ states. The increase in population ρ_{ff} is considerably weaker than ρ_{00}, in accordance with the spontaneous emission branching ratio of those two channels.

The strong oscillation dominates the temporal profiles in the SF time interval (200 fs–100 ps), where the strong SF pulse induces Rabi oscillation between the excited and final states accompanied by reabsorption and reemission, the Autler-Townes effect between states $\mathrm{He}^+(3p)$ and $\mathrm{He}^+(2s)$ leads to the splitting of the SF frequency. The excited state population is dumped as soon as the SF pulse train leaves the system. Although the rate of spontaneous emission $A_{3p,1s} = 6.48 \times 10^{-8}$ a.u. at the $|i\rangle \to |0\rangle$ transition is about 7 times faster than that $A_{3p,2s} = 8.67 \times 10^{-9}$ a.u.

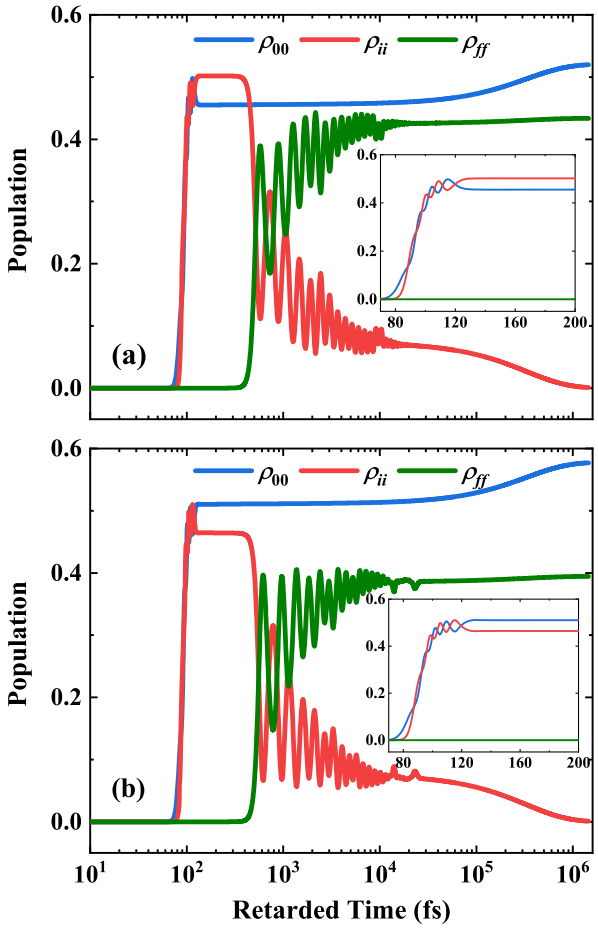

FIG. 3. Populations of the ionic states as a function of retarded time for $I_p = 5.5 \times 10^{14}$ W/cm^2 (a) and $I_p = 7.1 \times 10^{14}$ W/cm^2 (b) at $Z = Z_0 = 1$ mm. The population evolutions within the time window of the pump pulse (70–200 fs) are shown in the insets.

at the $|i\rangle \to |f\rangle$ transition (see SM, Note 4 [45]), the population $\rho_{00} \approx 0.45$ is essentially constant and thus small population inversion between states $|i\rangle$ and $|0\rangle$, together with the strong coupling of the $|i\rangle \to |f\rangle$ transition with SF radiation, the emission $|i\rangle \to |f\rangle$ dominates $|i\rangle \to |0\rangle$. This seemingly contradictory phenomenon can be explained in two ways. First, the SF generated at the $|i\rangle \to |0\rangle$ channel is characterized by $\tau_r = 0.0556$ ps, delay time $\tau_D = 2.66$ ps, and dephasing time $T_{\mathrm{DP}} = 2.20$ ps, which correspond to the damped SF regime (see SM, Note 2 [45]). Contrary to that, those parameters at the $|i\rangle \to |f\rangle$ transition correspond to the strongly oscillatory SF regime as it was shown above. That ensures the domination of the SF at the $|i\rangle \to |f\rangle$ channel. Second, comparison of the Einstein B coefficients for these two channels shows clearly that the stimulated emission at the transition $|i\rangle \to |f\rangle$ is 35 times higher than that of the $|i\rangle \to |0\rangle$ transition (see SM, Note 4 [45]), thus the stimulated emission at $|i\rangle \to |f\rangle$ is more likely.

In summary, we propose a strategy to measure Rabi oscillations induced by short wavelength XUV radiation

with the help of the followed superfluorescence spectra. Using the helium gas medium as an example, we theoretically study the stimulated emission from the $He^+(3p-2s)$ transition, pumped by the ultrashort intense XUV pulse on the $He^+(1s-3p)$ transition after the photoionization of He. The observed emission is proven to be a superfluorescence process, and the strongly oscillatory superfluorescence spectra imprint the Rabi oscillation and the saturation between state $He^+(3p)$ and $He^+(1s)$ driven by the pump pulse, which is reflected in the saturated shoulder peaks of the superfluorescence spectra. The proposed scheme suggests a feasible experimental method to capture Rabi oscillation and opens a potential route to sensitively probe other weak nonlinear optical effects in the XUV and x-ray regime.

Grants from NSFC (No. 11934004, No. 11974230, No. 12174009) are acknowledged. V. K. acknowledges financial support from the Swedish Research Council (No. 2019-03470).

*kimberg@kth.se
†song-bin.zhang@snnu.edu.cn

[1] I. I. Rabi, Phys. Rev. **51**, 652 (1937).
[2] S. H. Autler and C. H. Townes, Phys. Rev. **100**, 703 (1955).
[3] T. H. Stievater, X. Li, D. G. Steel, D. Gammon, D. S. Katzer, D. Park, C. Piermarocchi, and L. J. Sham, Phys. Rev. Lett. **87**, 133603 (2001).
[4] J. M. Martinis, S. Nam, J. Aumentado, and C. Urbina, Phys. Rev. Lett. **89**, 117901 (2002).
[5] H. Choi, V. M. Gkortsas, L. Diehl, D. Bour, S. Corzine, J. Zhu, G. Höfler, F. Capasso, F. X. Kärtner, and T. B. Norris, Nat. Photonics **4**, 706 (2010).
[6] Y. Dudin, L. Li, F. Bariani, and A. Kuzmich, Nat. Phys. **8**, 790 (2012).
[7] A. Feist, K. E. Echternkamp, J. Schauss, S. V. Yalunin, S. Schäfer, and C. Ropers, Nature (London) **521**, 200 (2015).
[8] N. V. Vitanov, A. A. Rangelov, B. W. Shore, and K. Bergmann, Rev. Mod. Phys. **89**, 015006 (2017).
[9] X. Xu, Z. Zhen, S. Jin, and J. Ren, Commun. Phys. **4**, 222 (2021).
[10] A. Blais, A. L. Grimsmo, S. M. Girvin, and A. Wallraff, Rev. Mod. Phys. **93**, 025005 (2021).
[11] H. Häffner, C. F. Roos, and R. Blatt, Phys. Rep. **469**, 155 (2008).
[12] I. Chiorescu, Y. Nakamura, C. J. P. M. Harmans, and J. E. Mooij, Science **299**, 1869 (2003).
[13] A. Gaita-Ariño, F. Luis, S. Hill, and E. Coronado, Nat. Chem. **11**, 301 (2019).
[14] E. Pedrozo-Peñafiel, S. Colombo, C. Shu, A. F. Adiyatullin, Z. Li, E. Mendez, B. Braverman, A. Kawasaki, D. Akamatsu, Y. Xiao, and V. Vuletić, Nature (London) **588**, 414 (2020).
[15] E. P. Kanter, B. Krässig, Y. Li, A. M. March, P. Ho *et al.*, Phys. Rev. Lett. **107**, 233001 (2011).
[16] S. Nandi, E. Olofsson, M. Bertolino, S. Carlström *et al.*, Nature (London) **608**, 488 (2022).
[17] W. Ackermann, G. Asova, V. Ayvazyan, A. Azima, N. Baboi *et al.*, Nat. Photonics **1**, 336 (2007).
[18] P. Emma, R. Akre, J. Arthur, R. Bionta *et al.*, Nat. Photonics **4**, 641 (2010).
[19] T. Ishikawa, H. Aoyagi, T. Asaka, Y. Asano *et al.*, Nat. Photonics **6**, 540 (2012).
[20] F. Gel'mukhanov, M. Odelius, S. P. Polyutov, A. Föhlisch, and V. Kimberg, Rev. Mod. Phys. **93**, 035001 (2021).
[21] K. J. LaGattuta, Phys. Rev. A **47**, 1560 (1993).
[22] M. G. Girju, K. Hristov, O. Kidun, and D. Bauer, J. Phys. B **40**, 4165 (2007).
[23] N. Rohringer and R. Santra, Phys. Rev. A **77**, 053404 (2008).
[24] L. S. Cederbaum, Y.-C. Chiang, P. V. Demekhin, and N. Moiseyev, Phys. Rev. Lett. **106**, 123001 (2011).
[25] P. V. Demekhin and L. S. Cederbaum, Phys. Rev. Lett. **108**, 253001 (2012).
[26] S. B. Zhang and N. Rohringer, Phys. Rev. A **89**, 013407 (2014).
[27] C. Weninger and N. Rohringer, Phys. Rev. A **90**, 063828 (2014).
[28] V. Kimberg and N. Rohringer, Phys. Rev. Lett. **110**, 043901 (2013).
[29] V. Kimberg and N. Rohringer, Struct. Dyn. **3**, 034101 (2016).
[30] J. R. Harries, C. Ohae, S. Kuma, K. Nakajima, T. Togashi *et al.*, Phys. Rev. A **94**, 063416 (2016).
[31] Š. Krušič, K. Bučar, A. Mihelič, and M. Žitnik, Phys. Rev. A **98**, 013416 (2018).
[32] Š. Krušič, K. Bučar, A. Mihelič, and M. Žitnik, Phys. Rev. A **99**, 013429 (2019).
[33] Š. Krušič, A. Mihelič, K. Bučar, A. Benediktovitch, S. Chuchurka, and M. Žitnik, Phys. Rev. A **107**, 013113 (2023).
[34] M. Nagasono, J. R. Harries, H. Iwayama, T. Togashi, K. Tono, M. Yabashi, Y. Senba, H. Ohashi, T. Ishikawa, and E. Shigemasa, Phys. Rev. Lett. **107**, 193603 (2011).
[35] J. R. Harries, H. Iwayama, S. Kuma, M. Iizawa, N. Suzuki, Y. Azuma, I. Inoue, S. Owada, T. Togashi, K. Tono, M. Yabashi, and E. Shigemasa, Phys. Rev. Lett. **121**, 263201 (2018).
[36] L. Mercadier, A. Benediktovitch, C. Weninger, M. A. Blessenohl, S. Bernitt *et al.*, Phys. Rev. Lett. **123**, 023201 (2019).
[37] R. Prakash and N. Chandra, Phys. Rev. A **24**, 962 (1981).
[38] P. P. Vasil'ev, Quantum Electron. **27**, 860 (1997).
[39] V. Kozlov, O. Kocharovskaya, Y. Rostovtsev, and M. Scully, Phys. Rev. A **60**, 1598 (1999).
[40] K. Sakoda and J. W. Haus, Phys. Rev. A **68**, 053809 (2003).
[41] R. Bonifacio and L. A. Lugiato, Phys. Rev. A **11**, 1507 (1975).
[42] R. Bonifacio and L. A. Lugiato, Phys. Rev. A **12**, 587 (1975).
[43] J. J. Maki, M. S. Malcuit, M. G. Raymer, R. W. Boyd, and P. D. Drummond, Phys. Rev. A **40**, 5135 (1989).
[44] L. Yuan, B. H. Hokr, A. J. Traverso, D. V. Voronine, Y. Rostovtsev, A. V. Sokolov, and M. O. Scully, Phys. Rev. A **87**, 023826 (2013).

[45] See Supplemental Material at http://link.aps.org/supplemental/10.1103/PhysRevLett.131.043201 for details, including additional references [46–56].
[46] A. J. Traverso, R. Sanchez-Gonzalez, L. Yuan, K. Wang, D. V. Voronine, A. M. Zheltikov, Y. Rostovtsev, V. A. Sautenkov, A. V. Sokolov, S. W. North, and M. O. Scully, Proc. Natl. Acad. Sci. U.S.A. **109**, 15185 (2012).
[47] R. Fleischhaker and J. Evers, Comput. Phys. Commun. **182**, 739 (2011).
[48] R. Friedberg and S. R. Hartmann, Phys. Rev. A **13**, 495 (1976).
[49] I. V. Hertel and C.-P. Schulz, *Atoms, Molecules and Optical Physics* (Springer, New York, 2014).
[50] F. Salvat, J. Fernández-Varea, and W. Williamson, Comput. Phys. Commun. **90**, 151 (1995).
[51] Y. Y. Qi, J. G. Wang, and R. K. Janev, Phys. Plasmas **23**, 073302 (2016).
[52] H. Marxer and L. Spruch, Phys. Rev. A **43**, 1268 (1991).
[53] K. Omidvar, At. Data Nucl. Data Tables **28**, 1 (1983).
[54] H. A. Bethe and E. E. Salpeter, *Quantum Mechanics of One- and Two-Electron Atoms* (Springer Science & Business Media, New York, 2012).
[55] Y. Y. Qi, J. G. Wang, and R. K. Janev, Phys. Rev. A **80**, 063404 (2009).
[56] L. B. Zhao and Y. K. Ho, Phys. Plasmas **11**, 1695 (2004).
[57] P. J. Singh, A. Shastri, R. Sampath Kumar, S. Jha, S. Rao, R. D'Souza, and B. Jagatap, Nucl. Instr. and Meth. A **634**, 113 (2011).